Online supplemental material

Congenic fine-mapping identifies a major causal locus for variation in the native collateral circulation and ischemic injury in brain and lower extremity

Robert Sealock PhD[1], Hua Zhang MD[1,3], Jennifer L. Lucitti PhD[1,3], Scott M. Moore MD[2] and James E. Faber PhD[1,3]

[1]Department of Cell Biology and Physiology, [2]Department of Surgery and [3]The McAllister Heart Institute, School of Medicine, University of North Carolina at Chapel Hill

Detailed materials and methods

Online Table I: Principle websites used

Online Table II: Genes in *Dce1*

Online Table III: Candidate SNPs in *Dce1*

Online Figure I: Detailed map of *Dce1*

Online Figure II: Pial collateral remodeling and hindlimb perfusion

Online Figure III: *Cln3*$^{-/-}$ mice

Online Figure IV: *Jmjd5*-engineered mice

Additional information on genes in *Dce1* having putative vascular roles not discussed in Discussion.

Online supplemental references

Detailed materials and methods

Congenic mice

The input strains to the congenic strains were BALB/cByJ (Bc; Jackson Laboratories stock no. 001026), CXB3/ByJ (CXB3; #000353) and CXB4/ByJ (CXB4; #000354). CXB3 and CXB4 are recombinant inbred lines derived from BALB/cByJ and C57Bl/6ByJ (B6; #001139). The very different distributions of blocks of B6 and Bc genotypes in CXB3 and CXB4 have been mapped in detail.[1] Of the 1078 genome-wide markers used in the mapping, 59.6% (CXB3) and 55.5% (CXB4) are the Bc allele. Congenic lines were generated using a speed congenics approach[2] by backcrossing CXB3 and CXB4 to Bc mice to give F1 mice. Starting at the second backcross (F1 to Bc; N2 generation), PCR markers (SNPs, simple sequence length polymorphisms, and restriction fragment length polymorphisms) in the blocks of B6 genotype were used to select for mice that lost the B6 genotype outside of *Candq1* but retained it within *Candq1*. Congenic lines from CXB3 and CXB4 were developed and maintained separately. Control B6 mice (C57Bl/6J; #000664) were obtained from Jackson Laboratories as new stocks and phenotyped contemporaneously with the congenic lines. The Mouse Phenome Database indicates no known genetic differences between BALB/c and BALB/cByJ strains in the region of interest in this study. Phenotyping of congenics and control B6 and Bc was done by a single observer (HZ). *Cln3*$^{\Delta ex7/8}$ mice[3] and *Cln3*$^{LacZ/LacZ}$ (Δ ex1-8)[4] (both on C57Bl/6J background) were from Jackson Laboratories (#017895) and Dr. Beverly Davidson, respectively. Mice genetically engineered at exon 4 of *Jmjd5* (B6 background) were from Dr. Takeshi Suzuki.[5] They were bred with B6-Cre mice[6] to produce mice null for *Jmjd5* in endothelial cells (*Jmjd5*$^{EC\Delta}$), globally haploinsufficient (*Jmjd5*$^{\Delta/+}$), or globally hypomorphic (*Jmjd5*$^{Neo/+}$). Gender does not influence collateral parameters,[7] thus cohorts were roughly half male and half female, and 2-3 months old. All animal procedures were approved by the University of North Carolina Institutional Animal Care and Use Committee.

Cerebral collateral visualization and morphometry

Filling of the pre-capillary pial circulation for counting and analysis of collateral diameters was as described previously in detail,[7] except that yellow Microfil was used instead of polyurethane.[8] Briefly, under deep anesthesia [ketamine (100mg/kg ip) and xylazine (15 mg/kg ip)], the circulation was flushed with PBS-heparin via retrograde cannulation of the abdominal artery, then maximally dilated with adenosine and papaverine. The dorsal calvarium and adherent dura mater were removed to allow visual control. The thoracic aorta was cannulated retrograde and yellow MicrofilR (FlowTech, Inc, Carver, MA) with viscosity adjusted to minimize entrance into capillaries was infused under a stereo microscope. The tissue was then fixed with topical 4% paraformaldehyde. On digital images (Leica MZ16FA, Bannockburn, IL) of the pial circulation, collaterals connecting the anterior cerebral (ACA) and middle cerebral (MCA) artery trees in both hemispheres were counted and measured for lumen diameter (ImageJ, NIH, Bethesda, MD), defined as the collateral diameter at its point halfway between the distal arterioles of the MCA and ACA tree that it cross-connects.

Middle cerebral artery occlusion and infarct volume

Permanent occlusion of the right MCA trunk by micro-cautery midway between the zygomatic arch and the pinna of the ear has been described in detail.[7,8] Briefly, mice were anesthetized with ketamine (100 mg/kg) and xylazine (10 mg/kg ip). A 4-5mm incision was made between the

right eye and ear, the temporal muscle was separated at its midpoint, and a ~2mm burr-hole over the trunk of the MCA in the right hemisphere was drilled with a handheld drill. The MCA was cauterized and transected, and the incision was closed. Mice received cephazolin and buprenorphine and were allowed to recover for 24 hours, then killed with an overdose of ketamine (100mg/kg ip) and xylazine (15 mg/kg ip). The brain was removed, cooled on dry ice until the tissue became stiff, and coronal slices (1mm) were incubated in 1% 2,3,5-tripenyltetrazolium chloride (TTC) in PBS at 37 degrees for 20 min, fixed with 1% PFA overnight. Infarct volume was calculated as the sum of the unstained volumes and expressed as a percent of total right cortical volume.[9]

Cerebral blood flow

24 hours after MCAO, mice were anesthetized (ketamine, 100 mg/kg) and retrogradely perfused via the thoracic aorta at 100 mmHg with PBS containing nitroprusside (0.1 mM) and papaverine (40 ug/ml) for maximal dilation for 2-3 minutes. 3×10^6 6 um diameter red-fluorescent 580/605 polystyrene FluoSpheres (Life Technologies) were sonicated vigorously and bolus-injected into the perfusion line just prior to the point of aortic cannulation and perfusion was continued for one minute. The brains were then removed, cooled on dry ice until the tissue became stiff, sliced (1 mm) and prepared for assessment of infarct volume as above and visualization of trapped microspheres by fluorescence microscopy. For each brain, microspheres in the infarct regions of the slices were counted in reverse-contrast images and summed. Density was calculated as the ratio of that count to the count in the corresponding zone on the contralateral, un-operated side.

Skeletal muscle collateral morphometry

Mice were anesthetized with ketamine (100mg/kg) and xylazine (10mg/kg), and heparinized. The heart was externalized through a partial sternotomy, with care not to damage the internal mammary arteries, aorta, and great vessels, as adequate abdominal wall filling requires patency of these vessels. A cardiotomy was then created in the left ventricle and a PE50 catheter with a tapered and flanged tip was inserted, with the tip positioned in the ascending aorta and secured with 6-0 suture placed around the aortic root. The heart was gently returned to its normal anatomic position prior to perfusion to prevent kinking of the aorta and its branches. Exsanguination and maximal dilation of the vasculature was accomplished with PBS containing sodium nitroprusside (40µg/ml) and papaverine (40µg/ml). Abdominal wall vasculature was then infused with Microfil (Flowtech, Inc, Carver, MA), with a composition of 8:1:1 (compound:diluent:curing agent) to optimize filling of the arterial and native collateral circulations while minimizing entrance into capillaries. Adequate and equivalent filling of each animal was ensured by hand-filling until Microfil first became visible within the femoral vein, which in pilot studies was shown to reliably reflect complete filling within the abdominal wall. Immediately after filling, 4% paraformaldehyde was instilled into the peritoneal cavity in order to fix the abdominal wall vasculature in the maximally dilated state. Following overnight fixation in 4% PFA, the abdominal wall musculature was dissected free from the viscera and overlying skin, and then underwent ethanol-based dehydration followed by methyl salicylate clearance to fully visualize filled abdominal wall vessels. Native collaterals were counted between the epigastric and iliolumbar arteries, as viewed from the peritoneal surface. Because slight differences in the completeness of filling was sometimes seen between the right and left sides, both sides were counted and the side with the most collaterals was used for data analysis. All vessel counting and data analysis was conducted in a blinded fashion.

Femoral artery ligation (FAL) and blood flow

Femoral artery ligation, laser Doppler flowmetry, and assessment of hindlimb use and ischemia appearance were assessed as described in detail.[10,11] Briefly, animals were anesthetized with ketamine (100 mg/kg im) and xylazine (15 mg/kg im). Hair was removed from the hindquarters with a depilating cream, with care taken to avoid erythema. Body temperature was maintained at 37.0 $\pm$ 0.5°C. The femoral artery was exposed aseptically through a 2-mm incision and isolated from the femoral vein and nerve, with care taken to avoid damage to vessels or nerve or retracting the incision. The femoral artery was ligated just proximal to the trifurcation of the genu, saphenous and popliteal arteries. The superficial epigastric artery was also ligated, but venous structures were left intact. The wound was irrigated with sterile saline, the incision was closed, and cefazolin (50 mg/kg im) and buprenorphine were administered. Blood flow was measured with a scanning laser-Doppler perfusion imager (model LDI2-IR, Moor Instruments, Wilmington, DE) that was modified for high resolution and depth of penetration (2 mm) with an 830-nm-wavelength infrared 2.5-mW laser diode, 100-_m beam diameter, and 15-kHz bandwidth. Animals were anesthetized with 1.125% isoflurane supplemented with 2:3 oxygen-air, and rectal temperature was closely maintained at 37.0 + 0.5°C.

The functional results of ischemia were assessed by use and appearance scores at days 1, 3, and 10 after femoral artery ligation. Animals were individually inspected for a foot appearance score or index of ischemia: 0, normal; 1–5, cyanosis or loss of nail(s), where the score is dependent on the number of nails affected; 6–10, partial or complete atrophy of digit(s), where the score reflects number of digits affected; 11, partial atrophy of forefoot. Hindlimb use scores (index of muscle function) were obtained by observation: 0, normal; 1, no toe flexion; 2, no plantar flexion; 3, dragging foot.[12]

Jmjd5-deficient mice

Mice harboring the floxed *Jmjd5* allele ($Jmjd5^{fl/fl}$), mice constitutively deficient in Jmjd5 ($Jmjd5^{\Delta/+}$), and mice hypomorphic for Jmjd5 ($Jmjd5^{neo/+}$) were generous gifts from Takeshi Suzuki.[5] To create a constitutive endothelial cell-specific Jmjd5 knockout, $Jmjd5^{fl/fl}$ mice were crossed with a *Cdh5*-Cre mouse (Jackson Laboratory, #006137) and backcrossed to $Jmjd5^{fl/fl}$ to produce $Cdh5\text{-}Cre^{+/-}$;$Jmjd5^{fl/fl}$ ($Jmjd5^{EC\Delta}$) mice.

Online Table I. Principle web sites used.

miRNA search: miRBase
http://www.mirbase.org/search.shtml
miRNA targets: TarBase 6.0
http://diana.imis.athena-innovation.gr/DianaTools/index.php?r=site/index
SNPs & Indels:
Jackson Laboratories Mouse Phenome database
http://phenome.jax.org/db/q?rtn=snp/ret1&uproj=CGD-IMP2&usampreg=1
Sanger Mouse Genomes Project
http://www.sanger.ac.uk/cgi-bin/modelorgs/mousegenomes/snps.pl
Sequence pileups for mouse strains: Sanger Mouse Genomes Project
http://www.sanger.ac.uk/cgi-bin/modelorgs/mousegenomes/lookseq/index.pl?show=1:10000000-10000000,paired_pileup&win=100&lane=129S1.bam&width=700
Non-synonymous SNP effect predictions:
Polyphen-2
http://genetics.bwh.harvard.edu/pph2/
Provean
http://provean.jcvi.org/seq_submit.php
Mouse phylogeny viewer
http://msub.csbio.unc.edu/
Gene and transcript lists:
NCBI map viewer
http://www.ncbi.nlm.nih.gov/mapview/maps.cgi?taxid=10090&chr=7&query=uid%28138 7727,7343204%29&QSTR=77035[gene_id]&maps=gene_set&cmd=focus
UCSC Genome Browser
http://genome.ucsc.edu/cgi-bin/hgGateway?clade=vertebrate&org=Mouse&db=0&hgsid=76761400
Synteny: NCBI homology maps
http://www.ncbi.nlm.nih.gov/projects/homology/maps/mouse/chr7/
Remapping between Builds 37 and 38 (remaps between mm9 and mm10)
http://www.ncbi.nlm.nih.gov/genome/tools/remap
Regulatory features search: Ensembl
http://useast.ensembl.org/Mus_musculus/Info/Index
Human GWAS studies of 16p11.2
http://www.genome.gov/gwastudies/
Long noncoding RNA database (mouse): NONCODE
http://159.226.118.44/NONCODERv3/index.htm
Relative expression levels: BioGPS
http://biogps.org/#goto=welcome

Online Table II: Genes in *Dce1*

Gene	Start location	
	Build 37	**Build 38**
Xpo6	7:133245232	7:126101718
Sbk1	7:133416133	7:126272619
Lat	7:133507341	7:126363827
Spns1	7:133513574	7:126370060
Nfatc2ip	7:133526368	7:126382854
Cd19	7:133551962	7:126408448
Rabep2	7:133572281	7:126428767
Atp2a1	7:133589374	7:126445860
Sh2b1	7:133610508	7:126466994
Tufm	7:133630869	7:126487355
Atxn2l	7:133635222	7:126491708
Eif3c	7:133690425	7:126546911
Cln3	7:133714914	7:126571400
Apobr	7:133728522	7:126585008
Il27	7:133732809	7:126589295
Nupr1	7:133766760	7:126623246
Ccdc101	7:133792823	7:126649309
Sult1a1	7:133816384	7:126672870
Slx1b	7:133832441	7:126688927
Bola2	7:133839514	7:126696000
Coro1a	7:133843288	7:126699774
Mapk3	7:133903140	7:126759626
Gdpd3	7:133909928	7:126766414
Ypel3	7:133920489	7:126776975
Tbx6	7:133924997	7:126781483
Ppp4c	7:133929382	7:126785868
Aldoa	7:133938748	7:126795234
Fam57b	7:133960399	7:126816885

Online Table III: Candidate SNPs in *Dce1*

Gene	*Identifier*	*Build 37*	*Build 38*	*B6*	*Bc*	*Consequence*
Xpo6	rs33063624	7:133295562	7:126152048	C	T	Intron
Xpo6	rs25093239	7:133307606	7:126164092	C	T	Intron
Xpo6	rs227712042	7:133338775	7:126195261	C	T	Intron
	rs33068721	7:133372819	7:126229305	A	G	Intergenic
	rs33072147	7:133380810	7:126237296	G	C	Intergenic
	rs33073821	7:133513295	7:126369781	C	G	Intergenic
Spns1	rs33077365	7:133516160	7:126372646	G	A	Intron
Nfatc2ip	rs33079501	7:133526623	7:126383109	G	A	3' UTR
	rs33078730	7:133561029	7:126417515	G	A	Intergenic
	rs243867849	7:133568397	7:126424883	G	A	Intergenic
	rs227824226	7:133569845	7:126426331	A	G	Intergenic
	rs246194872	7:133570124	7:126426610	C	A	Intergenic
	rs215526206	7:133570533	7:126427019	G	T	Intergenic
	rs259462571	7:133571315	7:126427801	C	T	Intergenic
Rabep2	rs236423818	7:133573990	7:126430476	C	A	Intron
Rabep2	rs258037007	7:133574019	7:126430505	A	G	Intron
Rabep2	rs261416329	7:133577552	7:126434038	C	T	Intron
Rabep2	rs33083620	7:133581943	7:126438429	C	T	Cs
Rabep2	rs33080487	7:133583723	7:126440209	G	A	Cn R298Q
Rabep2	rs254286371	7:133584920	7:126441406	A	G	Intron
Rabep2	rs213531450	7:133586656	7:126443142	T	C	Intron
Atp2a1	rs233753984	7:133591983	7:126448469	A	C	Intron
	rs227071387	7:133656437	7:126512923	G	T	Intergenic
	rs234324273	7:133687493	7:126543979	C	G	Intergenic
Cln3	rs33089967	7:133723863	7:126580349	G	A	Cn H120Y
	rs33092841	7:133747498	7:126603984	A	G	Intergenic
Nupr1	rs233244480	7:133769153	7:126625639	C	T	5' UTR

If the functional difference between B6 and Bc at *Dce1* should be attributable to one or more SNPs, the listed SNPs were judged to be candidates because they are present in Bc and AKR/J vs B6, but are not found in any of the high collateral number strains for which LookSeq pileup data is available (LP/J, C3H/HeJ, CAST/EiJ, CBA/J, DBA/J, FVB/NJ, NOD/ShiLtJ, and 129S1/SvImJ). An additional 42 SNPs found in Bc and AKR/J were judged not to be candidates because they are also present in one or more of the high collateral number strains.

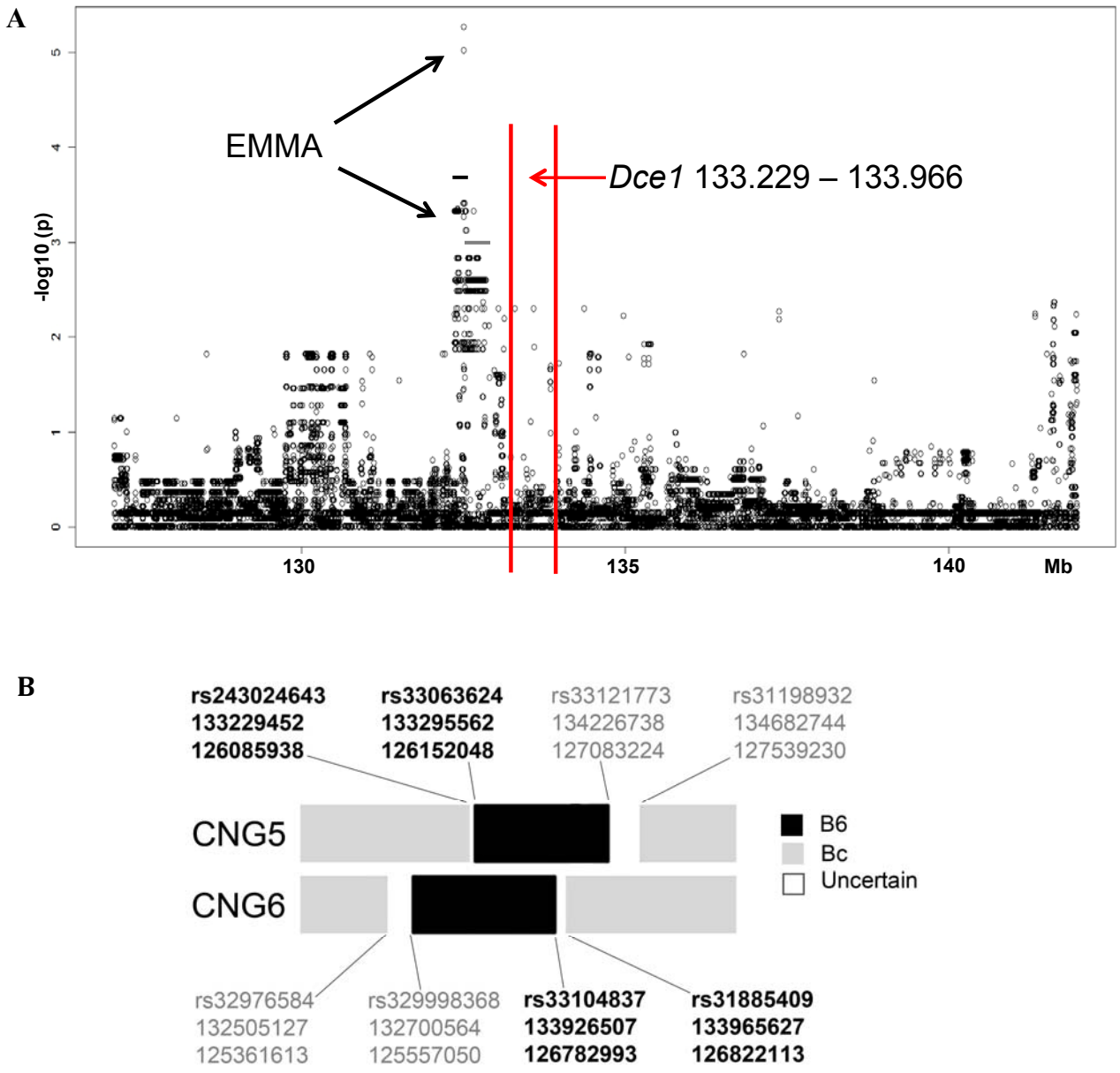

Online Figure I. **Maps of *Dce1***. **A**. EMMA and *Dce1* compared. The EMMA algorithm[13] was applied to *Canqd1* and 21 inbred mouse stains, yielding a highly significant peak at 132.356 to 132.817 Mb.[8,14] *Dce1* lies on the right shoulder of the EMMA peak, beginning at 133.229, or only 0.412 Mb further 3'. **B**. Detailed map showing the important markers (black text) that define *Dce1*, which is the zone of overlap between the introgressed regions of CNG5 and CNG6. B6 genotype is in black, Bc background genotype is gray, and regions of uncertain genotype between limiting markers are in white. Markers that delimit the introgressed regions outside of the overlap are in gray text. Locations in megabases beneath each marker are from MGSCv37 (mm9) (upper) and GRCm38 (mm 10) (lower).

A

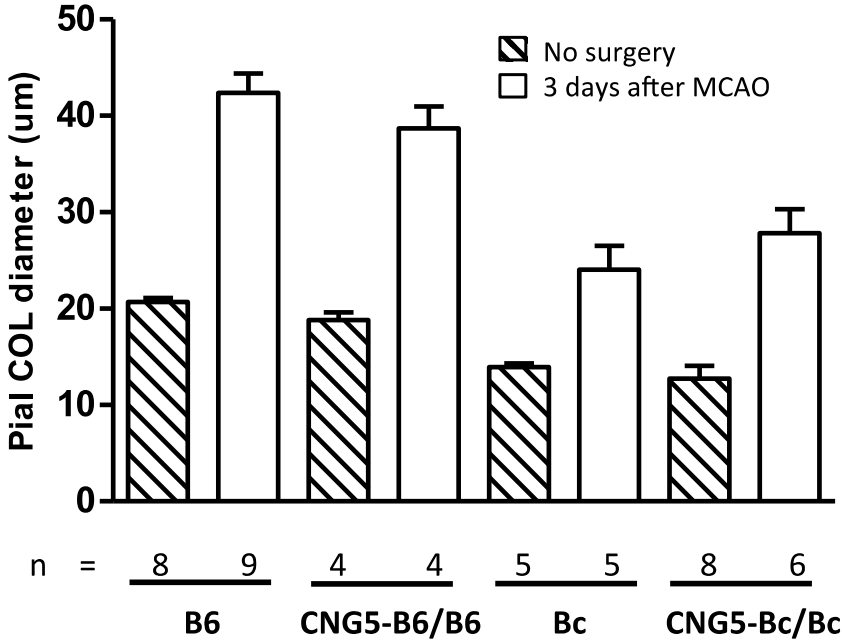

B	immediately after	day1	day3	day10
CNG5-B6/B6 (n=7-8)	**0.12**	**0.25**	**0.31**	**0.43**
CNG4-B6/B6 (n=10)	**0.11**	**0.19**	**0.31**	**0.44**

Online Figure II. Collateral remodeling (A) and recovery from FAL (B) in congenic and wild-type strains do not differ. A, Pial collateral remodeling. Hatched bars: baseline diameter prior to MCAO. Open bars: Remodeled diameter 24 hrs after middle cerebral artery occlusion (MCAO), which is maximal by day-3,[7] is comparable between CNG5 mice and the corresponding wild-types. This is expected since amount of remodeling is primarily determined by baseline collateral diameter (solid bars) before MCAO.[8] Wildtype data are from Zhang et al.[7] B, Laser-Doppler perfusion imaging values (perfusion units) after femoral artery ligation do not differ between CNG5- and CNG4-B6/B6 strains, and both are comparable to wild type C57BL/6 mice.[11] Values are mean ± SEM for n number of animals. B6, C57BL/6. Bc, BALB/c. Data for CNG4-B6/B6 are from Figure 5.

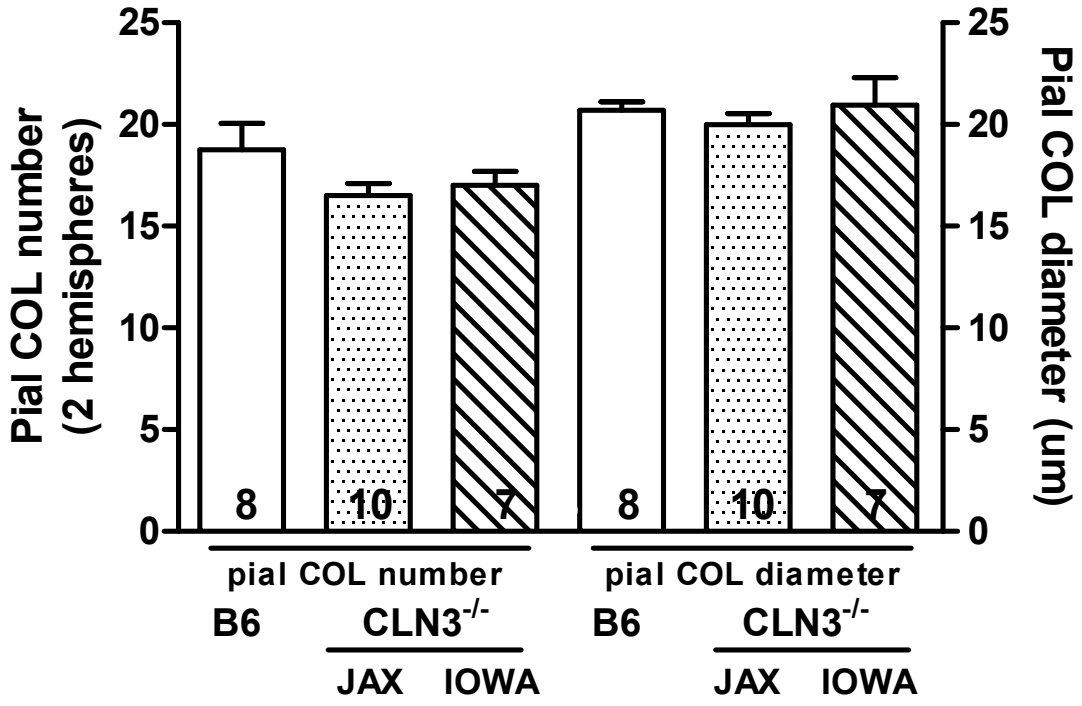

Online Figure III. Collateral number and diameter are not affected by absence of *Cln3*. Collateral number and diameter were measured in homozygous $Cln3^{\Delta Ex7/8}$ mice (JAX, stock number 017895, Jackson Laboratories)[3] and homozygous $Cln3^{\Delta Ex1-8}$ mice,[4] (IOWA, obtained from Dr. Beverly Davidson, University of Iowa), both stated by suppliers to be on the B6 background. See main text for further details. Neither parameter was significantly different from B6 control mice ($p \geq 0.1$ in all cases). Values in this and subsequent figures are mean ± SEM. Numbers of mice in this and subsequent figures are number of animals. JAX: 5 female and 5 male, 2-3 mos-age, 20-29 grams. IOWA: 4 male and 3 female, 2-7 mos-age, 23-35 grams.

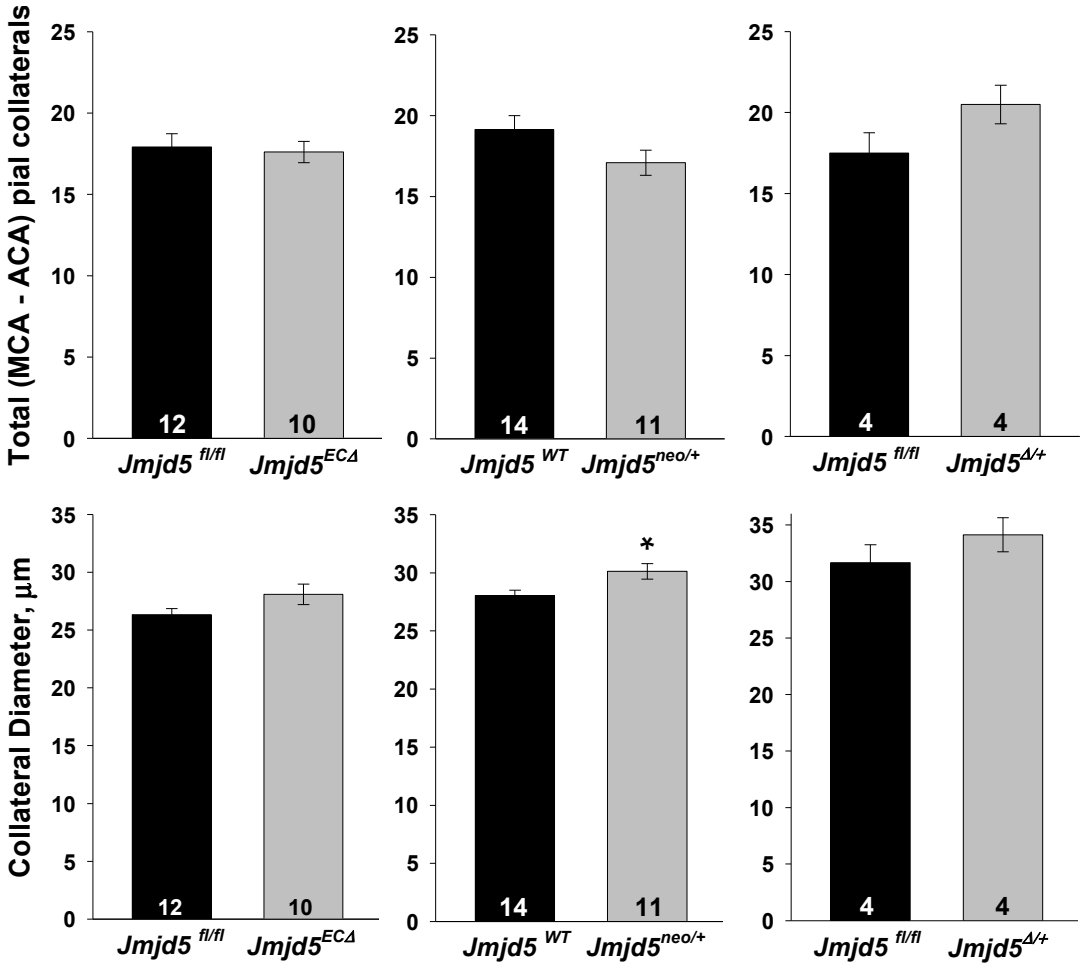

Online Figure IV. Differences in expression of *Jmjd5* do not impact collateral extent. *Jmjd5*$^{fl/fl}$, *Jmjd5*$^{neo/+}$ and *Jmjd5*$^{\Delta/+}$ were obtained from Dr. Takeshi Suzuki,[5] while *Jmjd5*$^{EC\Delta}$ mice were made from *Jmjd5*$^{fl/fl}$ mice at UNC (see Online Data Supplement – Detailed materials and methods). The cerebral vasculature of adult (3-4 month old) *Jmjd5*-engineered mice was filled with yellow Microfil^{TM} and analyzed as in "Cerebral collateral visualization and morphometry" above. Collateral number and diameter in both hemispheres were quantified in endothelial cell-specific knockout (*Jmjd5*$^{EC\Delta}$), global hypomorphic (*Jmjd5*$^{neo/+}$) and global haploinsufficient (*Jmjd5*$^{\Delta/+}$) mice and compared with wild-type littermates. Collateral number was similar in all groups. Although moderate *Jmjd5* knockdown (Jmjd5$^{neo/+}$) slightly increased collateral diameter compared to the wild-type littermate (*, $p<0.05$ by 2-tailed t-test), diameter was unchanged in the other groups. These data demonstrate that *Jmjd5* has negligible control over collaterogenesis, consistent with its physical location outside of *Dce1* (0.6 Mb 5' of *Dce1)*.

Additional information on putative candidate genes in *Dce1* not discussed in the main text.

SH2B1 (src-homology-2 adapter protein 1) is an SH2 domain-containing adapter protein for SRC and JAK2 kinases. SRC transduces signals from VEGFR2 leading to modulation of focal adhesions and VECadherin. Jak2 activation promotes endothelial cell migration and angiogenesis.[15] *SH2B1* is expressed at modest levels in most tissues, including endoglin-positive endothelial cells (BioGPS). Polymorphisms in an *SH2B1* obesity locus have been associated with reduced insulin-stimulated NO synthase activity in endothelial cells.[16]

Ppp4c is a serine, threonine phosphatase expressed in vasculature and other cells. Morpholino knockdown in zebrafish leads to intersegmental endothelial cell tracks that look normal but are not tubulated (ie, they don't accept blood from the dorsal aorta).[17]

APOBR is a receptor that binds to the apolipoprotein B48 of dietary triglyceride (TG)-rich lipoproteins. It is expressed in a variety of immune cells (neutrophils, macrophages, etc.) and at low levels in endothelial cells. The ApoB protein particle in ApoB-containing lipoproteins negatively regulates angiogenesis via downregulation of VEGFR1.[18] Multiple additional papers attest to the negative effects of ApoB on endothelial cells, but the receptor(s) is unknown.

Il-27 is a broadly active cytokine from immune cells and vascular smooth muscle cells. Numerous papers and reviews[19,20] attest to its roles in anti-angiogenesis, promotion of a proadhesive state for endothelial cells, "global changes in HUVEC gene expression in response to IL-27",[21] induction of anti-angiogenic CXCL9 and CXCL10 expression in endothelial cells, and pro-inflammatory actions.

Online References

1. Williams RW, Gu J, Qi S, Lu L. The genetic structure of recombinant inbred mice: High-resolution consensus maps for complex trait analysis. *Genome Biol*. 2001;2:research0046-research0046.18.
2. Wakeland E, Morel L, Achey K, Yui M, Longmate J. Speed congenics: A classic technique in the fast lane (relatively speaking). *Immun Today*. 1997;18:472-477.
3. Cotman SL, Vrbanac V, Lebel LA, Lee RL, Johnson KA, Donahue LR, Teed AM, Antonellis K, Bronson RT, Lerner TJ, MacDonald ME. Cln3(delta-ex7/8) knock-in mice with the common JNCL mutation exhibit progressive neurologic disease that begins before birth. *Hum Molec Gen*. 2002;11:2709-2721
4. Eliason SL, Stein CS, Mao Q, Tecedor L, Ding SL, Gaines DM, Davidson BL. A knock-in reporter model of batten disease. *J Neurosci.* 2007;27:9826-9834.
5. Ishimura A, Minehata K, Terashima M, Kondoh G, Hara T, Suzuki T. Jmjd5, an h3k36me2 histone demethylase, modulates embryonic cell proliferation through the regulation of cdkn1a expression. *Development*. 2012;139:749-759.
6. Lucitti JL, Mackey JK, Morrison JC, Haigh JJ, Adams RH, Faber JE. Formation of the collateral circulation is regulated by vascular endothelial growth factor-a and a disintegrin and metalloprotease family members 10 and 17. *Circ Res*. 2012;111:1539-1550.
7. Zhang H, Prabhakar P, Sealock R, Faber JE. Wide genetic variation in the native pial collateral circulation is a major determinant of variation in severity of stroke. *J Cereb Blood Flow Metab*. 2010;30:923-934.
8. Wang S, Zhang H, Dai X, Sealock R, Faber JE. Genetic architecture underlying variation in extent and remodeling of the collateral circulation. *Cir Res*. 2010;107:558-568.
9. Faber JE, Zhang H, Lassance-Soares RM, Prabhakar P, Najafi AH, Burnett MS, Epstein SE. Aging causes collateral rarefaction and increased severity of ischemic injury in multiple tissues. *Arteriosclerosis, thrombosis, and vascular biology*. 2011;31:1748-1756.
10. Chalothorn D, Moore SM, Zhang H, Sunnarborg SW, Lee DC, Faber JE. Heparin-binding epidermal growth factor-like growth factor, collateral vessel development, and angiogenesis in skeletal muscle ischemia. *Arterioscler Thromb Vasc Biol*. 2005;25:1884-1890.
11. Chalothorn D, Clayton JA, Zhang H, Pomp D, Faber JE. Collateral density, remodeling, and vegf-a expression differ widely between mouse strains. *Physiol Genomics*. 2007;30:179-191.
12. Chalothorn D, Faber JE. Strain-dependent variation in collateral circulatory function in mouse hindlimb. *Physiol Genomics*. 2010;42:469-479.
13. Kang HM, Zaitlen NA, Wade CM, Kirby A, Heckerman D, Daly MJ, Eskin E. Efficient control of population structure in model organism association mapping. *Genetics*. 2008;178:1709-1723.

14. Wang S, Zhang H, Wiltshire T, Sealock R, Faber JE. Genetic dissection of the canq1 locus governing variation in extent of the collateral circulation. *PloS one*. 2012;7:e31910.

15. Zhuang G, Wu X, Jiang Z, Kasman I, Yao J, Guan Y, Oeh J, Modrusan Z, Bais C, Sampath D, Ferrara N. Tumour-secreted mir-9 promotes endothelial cell migration and angiogenesis by activating the jak-stat pathway. *The EMBO journal*. 2012;31:3513-3523

16. Prudente S, Morini E, Larmon J, Andreozzi F, Di Pietro N, Nigro A, Gervino EV, Mannino GC, Bacci S, Hauser TH, Bellacchio E, Formoso G, Pellegrini F, Proto V, Menzaghi C, Frittitta L, Pandolfi A, Sesti G, Doria A, Trischitta V. The sh2b1 obesity locus is associated with myocardial infarction in diabetic patients and with no synthase activity in endothelial cells. *Atherosclerosis*. 2011;219:667-672

17. Kalen M, Wallgard E, Asker N, Nasevicius A, Athley E, Billgren E, Larson JD, Wadman SA, Norseng E, Clark KJ, He L, Karlsson-Lindahl L, Hager AK, Weber H, Augustin H, Samuelsson T, Kemmet CK, Utesch CM, Essner JJ, Hackett PB, Hellstrom M. Combination of reverse and chemical genetic screens reveals angiogenesis inhibitors and targets. *Chemistry & biology*. 2009;16:432-441

18. Avraham-Davidi I, Ely Y, Pham VN, Castranova D, Grunspan M, Malkinson G, Gibbs-Bar L, Mayseless O, Allmog G, Lo B, Warren CM, Chen TT, Ungos J, Kidd K, Shaw K, Rogachev I, Wan W, Murphy PM, Farber SA, Carmel L, Shelness GS, Iruela-Arispe ML, Weinstein BM, Yaniv K. Apob-containing lipoproteins regulate angiogenesis by modulating expression of vegf receptor 1. *Nature medicine*. 2012;18:967-973

19. Tartour E, Pere H, Maillere B, Terme M, Merillon N, Taieb J, Sandoval F, Quintin-Colonna F, Lacerda K, Karadimou A, Badoual C, Tedgui A, Fridman WH, Oudard S. Angiogenesis and immunity: A bidirectional link potentially relevant for the monitoring of antiangiogenic therapy and the development of novel therapeutic combination with immunotherapy. *Cancer metastasis reviews*. 2011;30:83-95

20. Demyanets S, Huber K, Wojta J. Vascular effects of glycoprotein130 ligands--part i: Pathophysiological role. *Vascular pharmacology*. 2012;56:34-46

21. Feng XM, Chen XL, Liu N, Chen Z, Zhou YL, Han ZB, Zhang L, Han ZC. Interleukin-27 upregulates major histocompatibility complex class ii expression in primary human endothelial cells through induction of major histocompatibility complex class ii transactivator. *Human immunology*. 2007;68:965-972